Quaternary International xxx (xxxx) xxx

Contents lists available at ScienceDirect

Quaternary International

journal homepage: www.elsevier.com/locate/quaint

Revisiting the Taman peninsula loess-paleosol sequence: Middle and Late Pleistocene record of Cape Pekla

S.N. Timireva [a], Yu.M. Kononov [a], S.A. Sycheva [a], N.A. Taratunina [a,b], P.I. Kalinin [c], K. G. Filippova [a], A.L. Zakharov [a], E.A. Konstantinov [a], A.S. Murray [d], R.N. Kurbanov [a,b,*]

[a] Institute of Geography, Russian Academy of Sciences, Staromonetny 29, 119017, Moscow, Russia
[b] Lomonosov Moscow State University, Leninskie Gory 1, Moscow, 119991, Russia
[c] Institute of Physical-Chemical, and Biological Problems of Soil Science, Russian Academy of Sciences, Institutskaya str., 2, 142290, Pushchino, Russia
[d] Nordic Laboratory for Luminescence Dating, Department of Earth Sciences, Aarhus University, DTU Risø Campus, DK-4000, Roskilde, Denmark

ARTICLE INFO

Keywords:
Loess
Paleosol
Pleistocene
Lithology
OSL-Dating
South east European plain

ABSTRACT

Loess deposits are widely spread all over Eastern Europe, extending as far south as the Sea of Azov and the northern Black Sea. For many decades these regions have been noted for series of key sections. However, despite prolonged investigations, a lack of absolute dating and detailed lithological data has left many unresolved problems in the correlation of the regional stratigraphic schemes. In this study, integrated studies were undertaken on the loess-paleosol sequence exposed on the northern coast of the Taman Peninsula, separating the Sea of Azov from the Black Sea. The exposure in the coastal scarp near Cape Pekla was sampled in detail for standard lithological and stratigraphic analyses, and for the first time, detailed data on the sediments lithology and petromagnetic properties were obtained, as well as the first optically stimulated luminescence age estimates. The data lead us to conclude that the formation of continental series exposed in the Pekla section started at the beginning of the Middle Pleistocene. There are five well pronounced buried soil complexes (PS 1–5) exposed in the sequence, covering sedimentation from the Middle Pleistocene to the present day. We attribute two lower paleosols (PS 4 and PS 5) to two main warm intervals of the Middle Pleistocene – MIS 9 and MIS 13, and the Kamenka interglacial paleosol, correlated with MIS 7 from other parts of the Azov loess area, is represented in the Pekla section by a sand layer formed at the time of the marine transgression dated to interval 220–280 ka (MIS 7). The upper soil horizons (PS1, PS2 and PS3) developed between 20 and 220 ka. The Pekla section contains a considerable proportion of sand fraction – presumably, due to active eolian processes that developed in immediate vicinities of sources of the material. The paleosol characteristics and the structure of loess horizons in the Pekla subaerial series differ considerably from the well described loess-paleosol series of the Northern Azov Sea coasts. In all probability, this region of the Taman Peninsula belongs to a specific province located south of the North Azov loess-soil province.

1. Introduction

Loess deposits cover about 10% of the global land surface (Pécsi, 1990; Muhs and Bettis, 2003). Loess thickness may vary from tens of centimetres to tens of meters, and the series often includes interlayers of buried paleosols. These loess and paleosol sequences (LPS) suggest essential changes of environments have occurred repeatedly in the past and present one of the most complete terrestrial natural archives recording global and regional climate changes (Kukla, 1987; Porter and An, 1995; Pye, 1995; Derbyshire et al., 1997; Stevens et al., 2007; Ryskov et al., 2008; Zykina and Zykin, 2008; Marković et al., 2011; Smalley et al., 2011; Sizikova and Zykina, 2015; Panin et al., 2019).

Most of the loess in Eurasia is confined to the latitudinal belt between 40° and 60° N, which covers most of the Quaternary periglacial regions. This is somewhat different in China, where loess occur in much lower latitudes remote from both continental ice sheets and alpine glaciers (Muhs and Bettis, 2003). While the Chinese loesses are exceedingly thick (hundreds of meters) and relatively localised, the loess of Eastern Europe is variable in thickness, but distinguished by its vast area (Velichko et al., 2017a,b,c).

* Corresponding author. Institute of Geography, Russian Academy of Sciences, Staromonetny 29, 119017, Moscow, Russia.
E-mail address: kurbanov@igras.ru (R.N. Kurbanov).

https://doi.org/10.1016/j.quaint.2021.06.010
Received 12 November 2020; Received in revised form 21 May 2021; Accepted 5 June 2021
Available online 19 June 2021

Loess deposition was the dominant sedimentation process in Eastern Europe during the Pleistocene. As a result, LPS are the most promising objects for the studies of paleoclimate fluctuations at a regional scale (Velichko, 1990; Velichko et al., 2000, 2011). Here, the authors concentrate their attention on the LPS of the Azov region (south of the East European Plain).

The southern coast of the Sea of Azov (Taman Peninsula) has been thoroughly studied since the early 20th century. N.I. Andrusov (1918, 1926, 1961) laid the foundation for the regional stratigraphy and geomorphology. Later on, I.M. Gubkin (1950) gave a detailed description of the regional stratigraphy and geomorphology. The first stratigraphic scheme of the Quaternary formations of the Taman Region was developed by G.F. Mirchink (1936) based on field studies of the natural exposures.

Since the early 2000s, the LPS of the Eastern Azov region have been continuously studied using an interdisciplinary approach under the guidance of A.A. Velichko, with the participation of specialists from Canada and China. The purpose of the studies was to reconstruct the climate and environments of the past and to predict their changes in future (over the 21st century) related to expected climate fluctuations (Timireva and Velichko, 2006; Velichko et al., 2009a, b, 2012, 2017; Liang et al., 2016; Chen et al., 2018a, b; Konstantinov et al., 2018; Panin et al., 2018). The surveys were mostly confined to the Taganrog Bay (the northeastern arm of the Azov Sea). The sequences studied in the many exposures in the region cover the major part of the Pleistocene. Each of the sections, however, includes some stratigraphic gaps, and so a comprehensive history of environmental evolution through the Pleistocene may be obtained only by comparison of data from all the key sites. In most of the sections, the Late Pleistocene part of the sequence lacks deposits datable to the MIS 3 interstadial (the time interval when the interstadial paleosol developed).

The southern coast of the Sea of Azov, in the north of the Taman Peninsula, is another region with well-developed series of LPS. Among the earliest comprehensive studies were works headed by A.A. Velichko in the early 1970s (Velichko et al., 1973b). Four paleosols were identified near Cape Pekla, and first paleomagnetic measurements and macromorphological descriptions performed.

In the early 2000s, research continued, mostly aimed at analyses of paleomagnetic characteristics (Pilipenko et al., 2005; Pilipenko and Trubikhin, 2011). No detailed studies of the Pekla sequence lithology have as yet been undertaken, and the absolute chronology data are insufficient.

The purpose of the present investigation was to reconstruct the conditions and dynamics of the sedimentation environment, as well as to determine the main chronological stages based on OSL dating.

2. Materials and methods

2.1. Study area

The studied region occupies the northwestern part of the Taman Peninsula, located between the Black Sea and the Sea of Azov (Fig. 1).

The Taman Peninsula is composed of Cenozoic sedimentary rocks, the total thickness of the latter amounts to approximately 2000 m (Shardanov and Borukayev, 1968). Quaternary deposits are widespread all over the region, dominated by loess-like loams alternating with paleosol horizons. Eluvial-deluvial, deltaic, lacustrine-marine (estuarine), lacustrine-fluvial, and fluvial deposits are also common.

The topography of the Taman Peninsula is distinct for numerous parallel hilly ridges and isolated hills up to 160–170 m high and 20–25 m long. The ridges are separated by low, flattened surfaces and extend towards the southwest. Occasional hills rise above the ridges. Depositional and depositional-erosional relief dominates in most of the Taman Peninsula (Potapov and Safonov, 1985). The synclinal lowered plains between ridges are filled with loams and clays deposited by slope-wash (deluvial) processes. The inter-ridge areas are completely levelled.

Fig. 1. Location of the studied Pekla section.

Structurally, the gently sloping loess plains are confined to synclinal and brachysynclinal depressions varying considerably in size and outline, and filled with thick unconsolidated deposits. Dune formations are typical for the lower parts of the loess plain near the coasts (Flerov, 1931). The sea coasts often form steep scarps up to 100 m high. Lakes or estuaries are often found in the topographic depressions within the coastal zone.

The Taman Peninsula and the Sea of Azov have a temperate continental climate, with a hot and dry summer and relatively mild and cloudy winter. The mean temperature is +25°C in summer and about 0°C in winter. Occasional short-term frosts freeze the soil to a depth of 5 cm at most. Mean annual precipitation is approximately 450–500 mm per year (Belyuchenko, 2010). Summer precipitation is predominantly stormy, in total about 250–300 mm. East winds dominate in winter and autumn, and variable winds (with some predominance of westerlies) are typical for summer. Northeastern and eastern winds can often result in dust storms, both in summer and winter.

Southern chernozems (or chestnut soils) cover most of the territory. The natural vegetation is represented by steppe and meadows. Aquatic plants occur in estuaries, and specific vegetation occupies sand beaches, solonchaks, and small patches under deciduous trees.

Our studies centred on a plot 3 km west of Kuchugury settlement on Cape Pekla (45° 25′56.1″ N, 36° 55′12.0″ E). The section is located on a high marine terrace (Fig. 2) forming a residual hill 337 m high confined between two gullies, near the side of a circular depression with stepped slopes. Several gullies have formed in the depression slope.

2.2. Sampling and laboratory measurements

The coastal scarp was cleaned of the outer dry and fissured layer 0.5–1.5 m thick. The macromorphology of the exposed sequence was described in detail, and samples taken for a complex of analyses at every 6 cm. Here we consider the results concerning the sediment lithology and age, namely grain size data, loss on ignition (LOI), magnetic susceptibility (MS), and optically stimulated luminescence (OSL).

Grain size analysis was made using a Malvern Mastersizer 3000

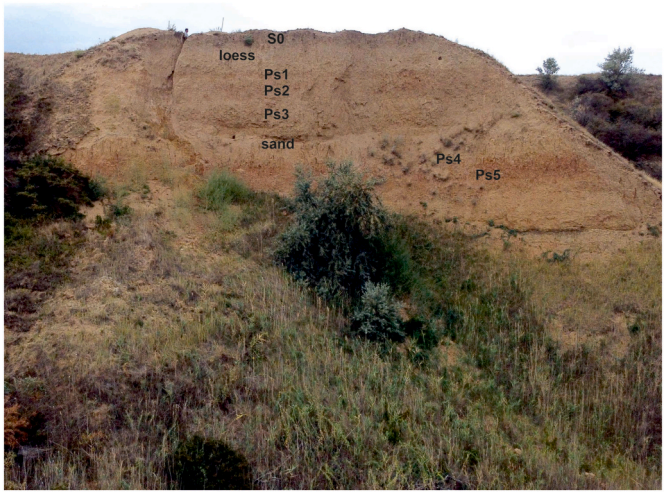

Fig. 2. The main stratigraphic units identified in the Pekla sequence.

laser diffractometer. Only the silicate component of the sediment, the most resistant to diagenesis, was analyzed; both organic matter and carbonates were removed during sample preparation. The latter included a sequential treatment of the sample with 20% solution of hydrogen dioxide (to remove organic matter), then 10% solution of hydrochloric acid (to remove carbonates), and finally with 4% solution of sodium pyrophosphate (to disperse the clay aggregates). The material was then transferred by pipette to a liquid tray in the material dispersion unit where it was subjected to ultrasonic at a power of 40 W for 100 s and intensely stirred at 2400 rounds per minute. After the ultrasonic treatment was complete, the grain size measurements were repeated ten times, and the results averaged using a Mastersizer v.3.62 application. The particle size distribution by fraction was calculated using the Fraunhofer approximation model.

The ***loss on ignition (LOI)*** was determined with the aim of estimating the content of organic matter and carbonates in the sample, which is important in the paleosol diagnostics. Following earlier work (Heiri et al., 2001; Bengtsson and Enel, 1986) the LOI values obtained at 550 °C show the organic matter content, while the difference between LOI values obtained at 950 °C and those at 550 °C (LOI 950 °C – LOI 550 °C) indicates the loss of carbonate CO_2. The samples, each of 10 ml in volume, were dried up for 12 h at 105 °C to remove all water (including hygroscopic). They were then incinerated in a muffle furnace under two temperature regimes (4 h at 550 °C and 2 h at 950 °C). The loss on ignition was found as the difference in weight before and after ignition using the electronic balance with the accuracy of 0.01 g. The resulting values formulas are:

$$LOI550 = \frac{DW105 - DW550}{DW105} \times 100;$$

$$LOI950 - 550 = \frac{DW550 - DW950}{DW105} \times 100,$$

where DW is dry weight.

Magnetic susceptibility (MS) measurements were performed using two methods. First, directly during field work on the wall of the section using a Zhinstruments SM30 field cappameter. Measurements were made at 6 cm intervals, the value was measured three times, and then averaged for each level. The second method was carried out in the laboratory with magnetic susceptibility meter ZH Instruments SM 150L. The presence (and amount) of paramagnetic and ferromagnetic substance in the deposits determine the MS value. The magnetic material may be introduced and/or develop in place as a result of chemical processes in the soil horizons (Maher, 1998). The highest MS values are usually found in the paleosols, while in the loess unaffected by soil processes it is at its minimum.

The samples were first dried in the furnace at 100 °C for 12 h to completely remove any hygroscopic moisture. Then a weighed portion of the sample (5 g) was placed in a cylindrical plastic container. The measurements were taken at an average frequency of 4118 Hz and the field strength of 80 A/m.

All the listed measurements were made in the Institute of Geography, RAS.

Luminescence dating. Four samples has been obtained from the Pekla section for absolute dating of the loess-paleosol series.

Samples were taken from the base of the modern soil (sample 200859), and from littoral sands correlatable with the Usunlarian transgression of the Pont (sample 200866) to build up a tentative chronostratigraphic scheme of the section. The samples were taken in lightproof plastic tubes; a standard technique was used in the section wall clearing and matching with the stratigraphic units. The samples were prepared for analysis in the Laboratory of Luminescence Dating (Moscow State University – Institute of Geography RAS) as follows: separation of the sand fraction (sieving); treatment of the grain-size fraction 90–180 μm with 10% hydrogen peroxide, hydrochloric acid, and finally hydrofluoric acid. Separation of quartz and feldspars grains was undertaken in a heavy liquid (polyvalent potassium tungstate) followed by additional cleaning of quartz grains with concentrated hydrofluoric acid (Kurbanov et al., 2019). Measurements of the equivalent dose and the dose rate were made in the Nordic Laboratory for Luminescence Dating, DTU Risø Campus.

The dose rate was calculated from the results of the sample activity measurements on a gamma-ray spectrometer (Table 1). A rather high content of radionuclides typical for subaerial loess-paleosol series was found, and the resulting dose rates vary around 3.3–3.5 Gy/ka.

The average water contents in the sequence were estimated from a consideration of the type of sediments (lesser values are typical of sands and greater – for loess), stratigraphic position in the sequence, and the duration of the groundwater influence and modern climate of the Taman Peninsula. The mean water content in the loess-paleosol series (the upper part of the sequence) is estimated at 13%, and that of littoral sands at 5% (Table 2).

The equivalent dose was measured for quartz (OSL) and feldspars (IR_{50} and $pIRIR_{290}$). The quartz OSL signal from sample 200859 was dominated by the fast-component (data not shown). The dose response curve was calculated from 5 points obtained as a result of fixed-dose irradiation from a beta source: 20, 40, 125, 0, and 20 Gy. The equivalent dose (D_e) for quartz in this sample is 48.3 ± 3.4 Gy (n = 17). Note that the quartz OSL signal for sample 200866 was in full saturation.

The measurements on feldspars were performed for 6–8 aliquots; the procedure included recording the luminescence response at temperatures 50 °C (IR_{50}) and 290 °C ($pIRIR_{290}$) for sample 200859, and IR_{200}-$pIRIR_{290}$ for 200866 (Buylaert et al., 2012), with laboratory dose: 250, 500, 1000, 0, 250 Gy. The dose measured on sample 200866 appeared to be close to complete saturation (931.8 ± 22.9 Gy). Two aliquots, however, seemed saturated (~1000 Gray), and therefore could be responsible for some underestimation of the calculated age.

3. Results

The main data obtained as results of field and laboratory works are combined in Fig. 3.

3.1. Section description

A complicated 11 m thick series of deposits of varying genesis – from marine to subcontinental and continental – is exposed in the upper part of the coastal outcrop (Fig. 2). Twenty-one layers have been identified altogether, and their morphology described (Fig. 3).

There are distorted layers of black clays of estuarine origin exposed at the base of the outcrop. The upper-lying subaerial part of the sequence

Table 1
Gamma-ray spectroscopy results. Radioactive element contents in the sample and the derived dose rate for quartz and K-rich feldspar.

Sample Code	Stratigraphy	^{238}U, Bq.kg^{-1}	^{226}Ra, Bq.kg^{-1}	^{232}Th, Bq.kg^{-1}	^{40}K, Bq.kg^{-1}	Dose rate, Gy.ka^{-1}	
						Quartz	Feldspar
200859	160	32 ± 4	38.2 ± 0.7	40.9 ± 0.5	446 ± 9	2.5 ± 0.1	3.5 ± 0.1
200866	670	32 ± 9	24.4 ± 0.7	27.2 ± 0.8	512 ± 13	2.4 ± 0.1	3.3 ± 0.1

Table 2
Results of luminescence dating of the Pekla section. WC – water conbtent, n – number of aliquots.

Sample Code	Stratigraphy	Depth, cm	Dose, Gy	n	Dose, Gy	n	Age, ka		WC
			Feldspar pIRIR290		Quartz		Feldspar pIRIR290	Quartz	
200859	B-carbonate layer of modern soil	160	230.9 ± 11.1	6	48.3 ± 3.4	17	66.8 ± 4.2	**19.2 ± 1.6**	13
200866	Marine sands	670	931.8 ± 108.2	8	in saturation		**279 ± 34**	in saturation	5

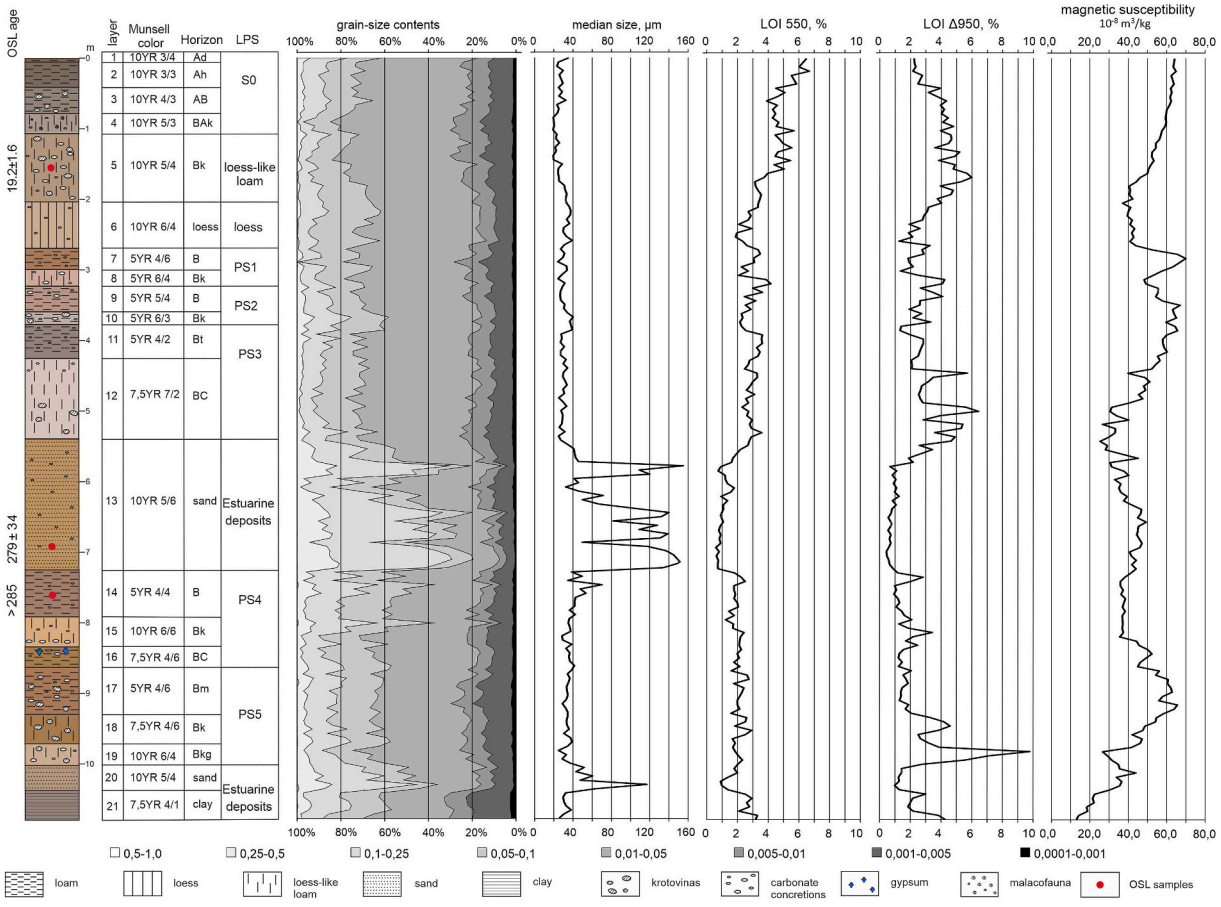

Fig. 3. Results of field and laboratory studies: stratigraphy of the Pekla section, grain-size composition, loss on ignition and magnetic susceptibility.

is composed mostly of loess-like deposits or loams bearing signs of active soil formation; it consists of two series separated with a sand layer, probably of marine genesis (beach facies). The lower subaerial series includes two paleosols, and the upper series, three. The lowermost (PS5) is composed of red-brown compact loam, nutty-platy in structure, with abundant Mn coatings and films in the pores and on aggregate facets. Mole burrows and calcareous concretions are abundant. The superimposed soil (PS4) consists of dark yellow medium loam of small-size rhombic structure, abounding in fine and medium-size pores. Humus-clay and clay coatings cover up the ped facets. Gypsum powdering and brown ferruginous films are found locally, as well as calcareous concretions up to 10 cm in size.

A thick layer of dark yellow sand penetrated with wormholes separates the lower subaerial layer from the upper one. There are occasional gypsum and carbonate pedofeatures.

The upper subaerial layer includes three paleosols. The lower of them (PS3) is composed of medium and light dark brown silty loam, with humus-clay coatings on the aggregate facets. Carbonate pedofeatures powder the clay coatings, with occasional small-size compact nodules (0.5–1 cm). The colour is most developed in the middle part of the layer. The middle paleosol (PS2) is dark grey-brown silty loam with brownish hue; the loam is finely porous, with prismatic structure, abounding in carbonate powder and pseudo-mycelium. The upper paleosol (PS1) occurs within the loess; it is a medium loess-like loam, brown with reddish hue, finely nutty and granular in structure. The paleosol is broken with sub-vertical fissures penetrating from the

overlying loess.

The top part of the sequence is composed of loess reworked in the upper layers by present-day processes of chernozem soil formation. The lower loess, without traces of soil development (pure loess), occurring immediately above the uppermost paleosol PS1 is a pale yellow sandy loam, finely porous and calcareous. A poorly humified horizon is traceable within the loess.

All paleosols are characterized by an eroded surface and loss of humus horizon, the former presence of which is confirmed by humus-clay cutans and krotovinas with a more humified filling than the host sediment. In the PS4 and PS3 profiles, the illuvial-clay horizon with humus-clay and clay cutans is clearly expressed. The loss of surface horizons of the paleosols is probably related to the active winds and growing aeolian activity in the periods preceding the subsequent loess deposition.

3.2. Grain size analysis

The silt fraction (0.005–0.05 mm) dominates in the Pekla section, its percentage varying from 16.5 (layer 13) to ~70.5% (layer 5). Percentage of clay (<0.005 mm) varies over the sequence from 4.3 to 23%, with the lowest concentrations in the sand horizon (layer 13). A slight increase in the clay content is recorded in horizon Bm of paleosol PS5 (layer 17) and the clay horizon at the base of the exposure (layer 21).

The total proportion of sand, including very fine (0.05–0.1 mm), fine (0.1–0.25 mm), and medium (0.25–0.5 mm) fractions, is quite considerable and varies along the sequence from 15.5% to 79.5%. The highest proportions of sand (34–79.5%) are found in the sand horizon (layer 13) and the horizon in the lower part of the section (layer 20), where the sand fraction proportion is as high as 55%. A noticeable increase in the sand fraction proportion (up to 38.5%) is recorded in the loess horizon (layer 6), as well as in the calcareous horizon of paleosol PS2 (layer 10) – up to 42%.

The analyses identifies four zones in the sequence, each characterized by a specific granulometric composition reflecting differences in deposition environments and post-sedimentary processes. Zone IV corresponds to the estuarine deposits forming the base of the sequence (layers 21-20). It usually contains a high proportion of fine-grained sand. The lower subaerial zone III (layers 19-14) and the upper zone I (layers 12–1) display many characteristics in common, in particular the dominance of the silt fraction, together with sand in considerable amounts. The latter may be due to sufficiently active aeolian processes during all stages of past and present sequence formation. Zone II (layer 13) features a marked predominance of sand fraction, which may be due to the transition to the estuarine regime of sedimentation. That horizon developed during a transgression, when the Black Sea level was rising due to thawing of alpine glaciers and increasing discharge of the rivers feeding the Black Sea basin (Fedorov, 1963). A considerable increase of the median grain size due to the fine fraction being washed-out from the beach sands characterises this horizon.

High median particle size values are also recorded in the sand layer at the base of the subaerial series – layer 20 (see Fig. 3). Over the rest part of the section, the median size is almost constant, with the only exception for a small peak recorded in the upper part of the Inzhavino paleosol (layer 14).

3.3. Loss on ignition

The LOI values at 550 °C (indicate the humus content in the soil) change from the base of sequence upwards and reach their maximum in horizon Ad of the modern soil (Fig. 2). In the lower part of the sequence slightly higher LOI values are recorded at horizon B levels in paleosols PS4 and PS5; the values drop noticeably in the overlying sandy horizon (layer 13), and increase again at the transition to paleosol PS3. In paleosols PS1 and PS2, the LOI 550 °C is practically the same as in PS3. A noticeable rise of LOI values was recorded in horizon Bk (layer 5) of the modern soil (PS0), and the maximum values are confined in the uppermost part of the sequence (layer 2). On the whole, however, the LOI values are not high and vary from 0.1% (layer 13) to 6.7% (layer 2).

The loss on ignition values at 950 °C (showing the carbonate content) vary widely over the sequence. The maximum values are recorded in the gley-carbonate horizon (Bgk) of paleosol PS5 (layer 19) which is composed of loess-like loam. The LOI values are 9.78%. The carbonates are present in a considerable amount (up to 6.44%) in the B horizon of paleosol PS3, which is composed of light loess-like loam and penetrated by numerous crotovinas (mole burrows). The upper loess deposits (layers 6-5) have LOI values up to 6%. The carbonate content drops markedly in the sandy horizon (layer 13), as indicated by an LOI 950 of 0.62%.

The analysis of the loss on ignition at 550 °C indicative of the degree of the soil humification bears witness to higher humus content in soil horizons than in loess. The humus content also increases upwards in the sequence, from older to younger paleosol, reaching its maximum in the modern soil.

The highest values of LOI at 950 °C, indicative of carbonate content, are found in loess and loess-like deposits.

3.4. Magnetic susceptibility (MS) record

The results of field and in laboratory measurements showed very high agreement (correlation coefficient 0.81). In the Pekla sequence, the mean values of the specific magnetic susceptibility are about 40×10^{-8} m^3/kg in loess and about 55×10^{-8} m^3/kg in paleosol horizons, compared to 65×10^{-8} m^3/kg in the modern (Holocene) soil (humus horizon). Characteristics similar to those in the modern soil are recorded in the paleosols PS2, PS3, PS5, where the specific magnetic susceptibility values average to 65×10^{-8} m^3/kg. Maximum values are recorded in paleosol PS1 (70×10^{-8} m^3/kg), minimum in the paleosol complex PS4 (40×10^{-8} m^3/kg).

A slight increase in the magnetic susceptibility index (up to 50×10^{-8} m^3/kg) in the sand layer 13 may indicate the contribution of marine sediments to the loess. However, this increase is negligible - it is comparable to the values of the magnetic susceptibility in the horizons of loesslike loams (layer 5). At the same time, attention is drawn to the absence of an increase in the magnetic susceptibility in the PS4 with values about $37 \times 10^{-8} m^3/kg$. This may be because the upper horizons of the PS4 soil (layers 14 and 15) are sandy and were eroded during marine transgression. As a result, the humus horizon was eroded and mixed with sand. This is evidenced by a decrease in the amount of silt and the increase of sand fractions in the upper horizon of the PS4 soil. Similar low values of the specific magnetic susceptibility index are recorded in the lower part of the PS3 paleosol (layer 12), which was formed in sandy marine sediments. This suggests that a change in the sediment source and the dilution of loesses with marine sediments leads to a decrease in the specific magnetic susceptibility index in paleosols. This is manifested in the paleosols formed immediately before and after the marine transgression.

Sandiness in the section is localised. With the exception of layers 13, 14, 15, nowhere else is the introduction of marine or other material recorded, either morphologically or granulometrically. Paleosol show maximum values of magnetic susceptibility (about $70–80 \times 10^{-8}$ m^3/kg, except for the low values of PS4), which corresponds to the pedogenic model of recording the magnetic susceptibility (Liu et al., 2008).

The results obtained by the magnetic susceptibility measurements proved its increase in the paleosols as well as in the modern soil. Enhanced soil formation processes could foster the recorded rise in MS during the warmer and wetter interglacial epochs. The bioclimatic factors promoted the formation of dispersed particles of ferrimagnetic minerals (magnetite, maghemite), which control the soil magnetic properties (Alekseev, 2003). The proportion of ferrimagnetic minerals indicates the climate present during soil formation. The mean annual rainfall reconstructions, based on rock magnetic characteristics obtained

from the loesses and paleosols, suggest that these layers formed under a semiarid climate. A negative correlation between the intensity of pedogenesis, expressed through MS, and the average particle size is observed in a number of loess sections in Europe and China (Marković et al., 2015; Liu et al., 2015). Such a correlation requires continuous sedimentation and the relationship is determined by a decrease in aeolian processes during soil formation, when the moisture increases and the surface stabilizes. However, such an ideal picture is not always observed in the loess-soil series. This may be explained by a hiatus in sedimentation or erosion of a part of the sedimentary sequence, or to local aeolian processes (on the sea coasts, for example, the Beglitsa section (Velichko et al., 2012, 2017a,b,c)), which are able to transport of silt and sand even in interglacial stages. In the coastal section of Pekla, the influence of both factors has likely influenced both grain size and the degree of pedogenesis. An increase in the magnetic susceptibility in the paleosol horizons has a positive correlation with the increase of the clay content (fraction of 0.001–0.005 mm) in the paleosol horizons as a result of pedogenic processes.

3.5. Analysis of chronological relationships

The uppermost sample 200859 dated by OSL on quartz and feldspars showed gives a pIRIR/Q ratio close to 3.5, which may be attributed either to a too short exposure of the grains, or to the material being mixed after its deposition, indicating that we cannot draw conclusions as to whether the quartz was well bleached at deposition (Murray et al., 2012). The quartz age is 19.2 ± 1.6 ka.

Of special interest is the age of the littoral sand (layer 13); based on the position in the sequence we correlate this with the Uzunlarian transgression of the Black Sea. The data available on the age of this transgression indicate the existence of a sea basin in MIS 7, that is 220–280 ka (Svitoch et al., 1998). A sample from the lower part of layer 13 is dated at 279 ± 35 ka, but the date may be underestimated. The dating results, along with properties of the deposits and their position in the sequence, allow layer 13 to be attributed to the initial phase of the Uzunlarian transgression of the Black Sea.

4. Discussion

Earlier investigations (Dodonov et al., 2006; Velichko and Morozova, 1973a; Velichko et al., 1973b, 1992; Velichko et al., 2017a,b,c) identified a number of paleosol and pedocomplexes in the Middle and Upper Pleistocene subaerial sediments on the coasts of the Sea of Azov and along the northern shores of the Black Sea; these paleosol can be correlated with interglacial and interstadial warming stages.

According to the generally accepted stratigraphic scheme of the Pleistocene, each period of cooling (glaciation) and warming (interglacial) corresponds to a certain MIS interval. However, and mainly as a result of the unsatisfactory absolute chronology of subaerial sequences, there are two current chronostratigraphic schemes for the East European Plain (Table 3). The differences between these two schemes arises in the period between MSI 5 and 13. In number of sections in the East European Plain, below the soil complex corresponding to the last interglacial (MIS 5), a so-called Romny paleosol is clearly distinguished. A.A. Velichko and his colleagues (Velichko et al., 2011; Velichko and Morozova, 2015), based on extended studies of loess-paleosol sequences on the East European Plain, concluded that the Romny paleosol formed during interstadial (see Table 3, option 1), in a period of relative warming within the Don glaciation (MIS 6). After MIS 12, the difference between the two variants disappears, and most researchers agree on the age of the Vorona paleosol complex formation (MIS 13–15).

However, some researchers identify the Romny paleosol as interglacial and correlate it with MIS 7 (see Table 3, option 2). This correlation leads to the 2nd chronological scheme (see Table 3) describing of the correlation between stratigraphic units and marine isotope stages (MIS) (Velichko and Morozova, 2010; Zastrozhnov et al., 2017); in that scheme, the Romny interstadial paleosol corresponds to MIS 7, and paleosols of the Kamenka and Likhvin interglacials – to MIS 9 and MIS 11 respectively.

According to the scheme suggested by Velichko and Morozova (2015), the following paleosols are recognized (corresponding to period os warming): Bryansk (Br), Mezin (Mz), Kamenka (K), Inzhavino (In), and Vorona (Vr). The uppermost – Bryansk – paleosol developed at the 2nd half of the Late Pleistocene, at the time of a relative warming (MIS 3), before the Last Glacial Maximum.

The next soil complex (Mezin) corresponds to MIS 5, its main phase being correlated with the Mikulino Interglacial (MIS 5e). It overlies the loess dated to the Middle Pleistocene cold phase and marks the Middle/Upper Pleistocene boundary. The Mezin paleosol is complicated in structure; it often consists of two or three horizons and has a polygenetic profile. The underlying Middle Pleistocene loess-paleosol series often includes two horizons of fossil soils. The principal phase of the upper

Table 3
The principal stratigraphic scheme of loess-paleosol sequence of the Brunhes epoch for the East European Plain and its correlation with marine oxygen isotope stages (according to Velichko and Morozova, 2010, 2015; Velichko et al., 2011).

Global Chronostratigraphy		Ice ages		Loess-paleosol succession	MIS	
Series	Subseries				Var.1	Var.2
Holocene		Recent Interglacial		Recent soil	1	1
PLEISTOCENE	LATE	Valdai glaciation	Late	Valdai loess	2	2
			Middle	Bryansk megainterval paleosol	3	3
			Early	Khotylevo loess	4	4
		Mikulino Interglacial		Mezin interglacial paleosol	5	5
	MIDDLE	Dnieper Glaciation		Dnieper loess	6	6
				Romny (?) interstadial paleosol		7
						8
		Kamenka (Chekalin) Interglacial		Kamenka interglacial paleosol	7	9
		Pechora Glaciation		Borisoglebsk loess	8	10
		Likhvin Interglacial		Inzhavino interglacial paleosol	9	11
		Oka Glaciation		Oka loess	10	12
					11	
					12	
		Ikorets Interglacial		Vorona paleosol complex	13	13
		glaciation			14	14
		Muchkap Interglacial			15	15
		Don glaciation		Don loess	16	16
		Okatovo interglacial		Rzhaksa interglacial paleosol	17	17
		Setun glaciation		Bobrov loess	18	18
	Brunhes-Matuyama boundary					

Middle Pleistocene paleosol is correlated with the Kamenka Interglacial (MIS 7). The main phase of the Middle Pleistocene Inzhavino paleosol developed in the Likhvin Interglacial (MIS 9). The oldest paleosol found in several adjacent sections exposing the Pleistocene LPS is Vorona paleosol, its principal phase being correlated with the Muchkap Interglacial (MIS 15).

The materials obtained by the authors of the present paper in the process of the stratigraphic studies of the Pekla section are in reasonable agreement with the earlier investigations carried out by A.A. Velichko and his colleagues (Velichko et al., 1973b), as well as with materials obtained by other authors (Pilipenko et al., 2005; Dodonov et al., 2006; Pilipenko and Trubikhin, 2011) who worked on the same part of the coast. It is noteworthy that the slope erosion processes (landslides, rockfalls, etc.) are exceedingly active in the coastal zone of the region. This explains why sequences studied at different times were described in different parts of the long coastal outcrop near the actively eroding Cape Pekla. As a result, section descriptions differ to a certain extent in structure. The newly described part of the section and previously described parts of the outcrop together with the Tsokur site located in the central part of the Taman peninsula are generalized in the correlation chart (Fig. 4).

The paper by Velichko et al. (1973b) provides information on four sections laid over a length of 2 km east of Cape Pekla and is notable for the stratigraphic persistence of the loess-soil series and a strong resemblance not only in their number, but also in specific features of the facial transitions. Two sections were sampled for paleomagnetic measurements at 0.5–1 m intervals. All the samples were normally magnetized, which was advanced as an argument in favour of the entire continental series having been deposited during the Brunhes epoch of normal polarity. It is also stressed in the paper that, as follows from the marine fauna studies by P.V. Fedorov (1963), the estuarine-marine deposits underlying the subaerial part of the sequence yielded species attributed to the Tiraspolian faunal assemblage and corresponding to MIS 17 in age.

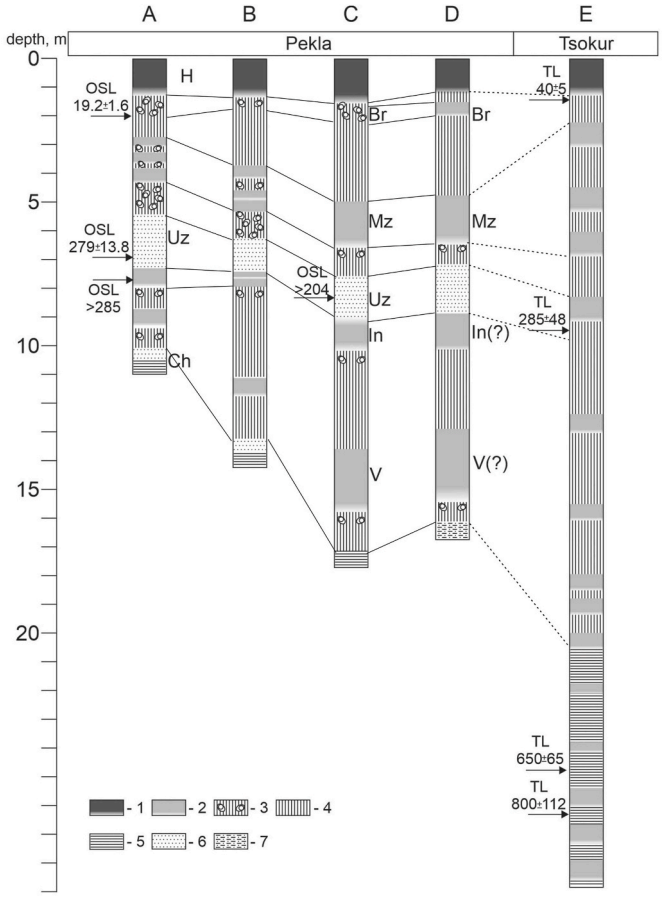

Fig. 4. Correlation chart of the previously described parts of the Pekla cape coastal outcrop and newly studied section with the central Taman peninsula Tsokur site. A – this study; B – Velichko et al. (1973b), C – Pilipenko et al. (2005); D – Dodonov et al. (2006); E – Zubakov (1988). Stratigraphic subdivisions: H – Holocene: Br – Bryansk paleosol; Mz – Mezin pedocomplex; In – Inzhava paleosol; V – Vorona paleosol; Uz – Uzunlar transgression of the Black sea; Ch – Chaudian-Bakunian transgression. Sediment type: 1 – modern soil; 2 – paleosols; 3 – illuvial carbonate unit; 4 – loess; 5 – clay; 6 – sand; 7 – silt.

The papers by A.E. Dodonov and colleagues (Dodonov et al., 2006) and by A.K. Markova (2002) gave a description of small mammal remains recovered from alluvial and lagoon deposits underlying the Vorona paleosol (PS5). These fauna corresponds to the Tiraspolian faunal assemblage, which lends support to the early Middle Pleistocene age of the deposits underlying the subaerial formation. The faunal remains are comparable in composition to the Tiraspolian faunal assemblage (MIS 17). Thus all these researchers agree that the strata at the base of the Pekla section was formed during a marine transgression that occurred approximately 700–650 thousand years ago (Zubakov, 1989), corresponding to MIS 17.

Several papers (Pilipenko et al., 2005; Pilipenko and Trubikhin, 2011) consider results of thorough stratigraphic and petromagnetic analyses performed on the extensive collection of LPS samples taken from the Pekla sequence using continuous sampling. Based on the correlation between the magnetic susceptibility and relative changes of the oxygen isotope $\delta^{18}O$, the authors of the earlier investigations compared the maximums of the SPECMAP curve showing relative changes in the oxygen isotope (Bassinot et al., 1994) with changes in the residual magnetization of LPS measured in the Pekla sequence. These authors observed a marked similarity between the two curves, providing the possibility of correlating the warm intervals (odd-numbered marine isotope stages) with increases in the concentration of magnetic minerals (carriers of residual natural magnetization) confined mostly to paleosol horizons. In this way, the uppermost soil complex in the sequence was correlated with MIS 5 and denoted Mezin. In addition, a single sample was taken for feldspar OSL dating from the middle part of the sand layer (corresponding to layer 13 in our description of the sequence). The dating (also performed at Aarhus University) gave a minimum OSL age of 204 ka BP, pointing to the most probable timing of the deposition of these sandy deposits during MIS 7.

No less important, although undertaken some time ago, are results of studies on another key section on the Taman Peninsula, situated about 30 km south of the Pekla Cape. This is a coastal scarp at the southern end of the Tsokur Lake (Geochronology of the USSR, 1974; Zubakov, 1988).

Fourteen paleosols described in the section varied in colours (from yellow-grey to bright red). They were separated with light-coloured loams, mostly with a well-developed carbonate horizon at the top. No visible gaps were recorded between the layers. It was noted that the soil profiles are poorly differentiated; the clay content, carbonate content, and red colour intensity grow regularly downward.

A few layers were dated by thermoluminescence, the lowermost sample taken from under the 12th paleosol was dated to 800 ± 112 ka. The age of deposits separating the 11th and 12th paleosols were 650 ± 65 ka. The next sample taken at a level of the 4th paleosol showed the age of 285 ± 48 ka. The youngest sample, 40 ± 5 ka, refers to the uppermost loess horizon (above the 1st paleosol).

From a comparison between the data on age and stratigraphy of the Tsokur and Pekla sequences, we conclude relative agreement between both sections, at least in the upper part (Tsokur).

Thus, both new data and the results of previous studies allows us to state that the two lowermost paleosol of the Pekla section of 2019 (PS 4 and PS 5) were formed in the period from ~300 to ~600 ka (MIS 9–15); they are both located between two reliably dated horizons (layers 13 and 20, 21). The lower part of the section (layers 20 and 21), represented by estuarine deposits, corresponds to MIS 17 (see above). Layer 13

consists of sands and, according to the new OSL ages, formed ~280 ka ago, corresponding to the end of MIS 8.

According to variant 1 of the chronostratigraphic scheme for the East European Plain (Table 3), two paleosol complexes, Inzhavino and Vorona, were formed between the cooling periods of MIS 8 and MIS 16, during interglacial periods. That is, although 4 interglacials occurred during this period, only two warm periods were reflected in the Pekla LPS. This situation is also observed in other outcrops located nearby. Therefore, it is difficult at this stage to match Vorona and Inzhavino paleosols to a specific MIS. It should be noted that in the part of the Pekla section described here, PS 4 is eroded directly above PS 5, while during previous field studies (Pilipenko et al., 2005; Dodonov et al., 2006; Pilipenko and Trubikhin, 2011) a loess layer of 0.7–1 m thickness was described between these two paleosols.

Even though probably underestimated, the age of the deposits of layer 13 of 279 ± 35 ka is an important result. This age allows the determination of the time of sedimentation during the initial phase of the Uzunlar transgression of the Black Sea. This horizon of the Pekla section is an analogue of the Kamenka paleosol of the Southern East European plain that developed during MIS 7.

The ages of the upper three paleosols (PS1, PS2, and PS3) are much weaker than those of the underlying layers, but as a result of the ages from layers 5 (19.2 ± 1.6 thousand years) and 13 (279 ± 13 thousand years), it can be assumed that loess-paleosol series in the interval of 2–5 m were formed in the period 20–220 thousand years ago (MIS 3–6). At this stage, it is difficult to pinpoint the exact age of PS1, PS2, and PS3. It is most likely that PS3 formed in the warmest phase of the last interglacial (MIS 5e) and is part of the Mezin pedocomplex, characterized by a two and sometimes three-membered structure. Accordingly, there are two options: in the Pekla section we either have a three-membered Mezin pedocomplex and then PS1 and PS2, like PS3, belong to MIS 5, or this pedocomplex consists of two horizons in which only PS2 and PS3 are included. In the second variant, PS1, most likely, should be identified as Bryansk paleosol corresponding to MIS 3. Thus, more detailed OSL dating of the upper part of the sequence is needed for a reliable cronostratigraphic description of the loess-paleosol sequences of the Taman peninsula.

The high values of the magnetic susceptibility index in the PS1 paleosol are notable, especially if we refer it to MIS 3. Such high values are not typical for MIS 3 in the Azov Sea region and in the central part of the East European Plain (Panin et al., 2018). However, in the Roksolany section, which is located in the Black Sea lowland of Southern Ukraine, MIS 3 has a high magnetic susceptibility value, comparable to MIS 5 (Hlavatskyi et al., 2020). In general, the values of the magnetic susceptibility correlate fairly well with the Roksolany section, where the values slightly increase in the upper part of the section. The difference is that in the Pekla section there are no pronounced peaks of magnetic susceptibility in the middle part of the profile (MIS7 and MIS 9). (But these deposits are sandy as a result of the Uzunlar basin marine transgression during this period). The similarity of the petromagnetic properties of the loess-paleosol series of the northwestern Black Sea area and the northern Black Sea coast indicates similar climatic conditions in this region during the Pleistocene.

5. Conclusion

For the first time the complex series of subaerial and marine sediments at Cape Pekla have been described and studied using sedimentological and rock magnetic methods. We provide new OSL ages that provide a basis for understanding the complicated stratigraphy of the Pekla sequence. Based on our integrated studies, together with earlier results, the beginning of the continental series of the Pekla sequence is dated to the early Middle Pleistocene. Despite possible gaps in a deposition, the Pekla sequence includes all the main horizons correlatable with global climate changes of the Middle and Late Pleistocene, including subaerial loess-paleosol sequence and marine sediments of the Uzunlar transgression of the Black sea.

The loess-soil series of the Taman Peninsula appear to have considerable promise for tracing climate and environment changes through the Pleistocene. Future work should be centred on the dating of deposits, particularly those of the upper part of the sequence (paleosols PS1, PS2 and PS3); OSL and AMS dating studies of small mammals represents a promising possibility for the creation of a reliable chronostratigraphic chart of the Taman loess region.

Author contributions SNT, YMK and RNK – conducted the field work, conceptualized stratigraphy and regional correlations, co-wrote the original draft, acquired funding, SAS – participated in the field work and performed a paleopedological description and interpretation; NAT and ASM – performed OSL dating; EAK – performed grain size analyses; PIK and ALZ – performed rock magnetic measurements and interpretations; KGF – created the stratigraphic charts, compiled and translated literature. All co-authors contributed to data interpretation in their respective fields of expertise and provided critical revision to the manuscript.

Data availability

All data generated or analyzed during this study and supporting the findings of this study are included in this published article and its supplementary information files.

Declaration of competing interest

The authors declare that they have no known competing financial interests or personal relationships that could have appeared to influence the work reported in this paper.

Acknowledgements

The reported study was funded by Russian Foundation for Basic Research (project number 18-55-91010: field research, rock magnetic and stratigraphic correlations), and within the framework of the state-ordered research theme of the Institute of Geography RAS (no. 0148-2019-0005: grain-size analyses). Luminescence dating and RNK was supported by Russian Science Foundation, project № 19-77-10077. We are grateful to our colleague Dr. A.K. Markova for consultations.

References

Alekseev, A.O., Alekseeva, T.V., Maher, B.A., 2003. Magnetic properties and mineralogy of iron compounds in steppe soils. Eurasian Soil Sci. 36, 59–70.

Andrusov, N.I., 1918. Geological structure of the Kerch strait bottom, 12 Izvestiya Akademii Nauk SSSR. Ser. 6 (1), 23–28 (In Russian).

Andrusov, N.I., 1926. Geological structure and history of the Kerch strait, 3/4. In: Bull. MOIP. GEOL., vol. 34, pp. 294–332 (In Russian).

Andrusov, N.I., 1961. Selected Works. Academy of Sciences of USSR, Moscow, pp. 621–627 (In Russian).

Bassinot, F.C., Labeyrie, L.D., Vincent, E., et al., 1994. The astronomical theory of climate and the age of the Brunhes-Matuyama magnetic reversal. Earth Planet Sci. Lett. 126, 91–108. https://doi.org/10.1016/0012-821X(94)90244-5.

Belyuchenko, I.S., 2010. Ecology of the Krasnodar Region (Regional Ecology). Krasnodar, Kuban State Agrarian University, p. 355.

Bengtsson, L., Enell, M., 1986. Chemical Analysis. In: Berglund, B.E. (Ed.), Handbook of Holocene Palaeoecology and Palaeohydrology. John Wiley & Sons Ltd, Chichester, pp. 423–451.

Buylaert, J.P., Jain, M., Murray, A.S., Thomsen, K.J., Thiel, C., Sohbati, R., 2012. A robust feldspar luminescence dating method for Middle and Late Pleistocene sediments. Boreas 41 (3), 435–451. https://doi.org/10.1111/j.1502-3885.2012.00248.x.

Chen, J., Yang, T.B., Matishov, G.G., Velichko, A.A., Zeng, B., He, Y., Shi, P.H., 2018a. Luminescence chronology and age model application for the upper part of the Chumbur-Kosa loess sequence in the Sea of Azov, Russia. J. Mt. Sci. 15, 504–518. https://doi.org/10.1007/s11629-017-4689-0.

Chen, J., Yang, T.B., Matishov, G.G., Velichko, A.A., Zeng, B., He, Y., Shi, P.H., Fan, Z., Titov, V.V., Borisova, O.K., Timireva, S.N., Konstantinov, E.A., Kononov, Y.M., Kurbanov, R.N., Panin, P.G., Chubarov, I.G., 2018b. A luminescence dating study of loess deposits from the Beglitsa section in the Sea of Azov, Russia. Quat. Int. 478, 27–37. https://doi.org/10.1016/j.quaint.2017.11.017.

Derbyshire, E., Kemp, R.A., Meng, X., 1997. Climate change, loess and paleosols: proxy measures and resolution in North China. J. Geol. Soc. 154, 793–805. https://doi.org/10.1144/gsjgs.154.5.0793.

Dodonov, A.E., Zhou, L.P., Markova, A.K., Tchepalyga, A.L., Trubikhin, V.M., Aleksandrovski, A.L., Simakova, A.N., 2006. Middle–upper Pleistocene bio-climatic and magnetic records of the northern Black sea coastal area. Quat. Int. 149, 44–54. https://doi.org/10.1016/j.quaint.2005.11.017.

Fedorov, P.V., 1963. Stratigraphy of Quaternary Deposits of the Crimean-Caucasian Coast and Some Questions of the Geological History of the Black Sea. Academy of Sciences of the USSR, Moscow, p. 164 (In Russian).

Flerov, A.F., 1931. Sandy landscapes of the Black Sea-Azov coast of the Caucasus, their origin and development. Izvestiya Rus. Geogr. Obschestva LXIII (1), 21–42 (In Russian).

Geochronology of the, U.S.S.R., 1974. The Late Pliocene and Quaternary, vol. 3, p. 358 (In Russian).

Gubkin, I.M., 1950. Review of Geological Formations of the Taman Peninsula. In: Selected Works. Academy of Sciences of the USSR, Moscow, pp. 139–167 (In Russian).

Heiri, O., Lotter, A.F., Lemcke, G., 2001. Loss on ignition as a method for estimating organic and carbonate content in sediments: reproducibility and comparability of results. Paleolimnology 25, 101–110. https://doi.org/10.1023/A:1008119611481.

Konstantinov, E.A., Velichko, A.A., Kurbanov, R.N., Zakharov, A.L., 2018. Middle to late Pleistocene topography evolution of the north-eastern Azov region. Quat. Int. 465 (A), 72–84. https://doi.org/10.1016/j.quaint.2016.04.014.

Kukla, G., 1987. Loess stratigraphy in Central China. Quat. Sci. Rev. 6 (3–4), 191–207. https://doi.org/10.1016/0277-3791(87)90004-7, 209-219.

Kurbanov, R.N., Yanina, T.A., Murray, E.S., Semikolennykh, D.V., Svistunov, M.I., Shtyrkova, E.I., 2019. Age of the Karangat Transgression of the Black Sea, vol. 6. Bulletin of the Moscow University, Geography Series, pp. 29–40.

Liang, Y., Yang, T.B., Velichko, A.A., Zeng, B., Shi, P.H., Wang, L.D., He, Y., Chen, J., Chen, Y., 2016. Paleoclimatic record from Chumbur-Kosa section in Sea of Azov region since marine isotope stage 11. J. Mt. Sci. 13, 985–999. https://doi.org/10.1007/s11629-015-3738-9.

Maher, B.A., 1998. Magnetic properties of modern soils and Quaternary loessic paleosols: paleoclimatic implications. Palaeogeogr. Palaeoclimatol. Palaeoecol. 137, 25–54. https://doi.org/10.1016/S0031-0182(97)00103-X.

Markova, A.K., 2002. New findings of fossil small mammals on the Taman peninsula. Third all-Russian conference of quaternary research. Smolensk 1, 166–167.

Marković, S.B., Hambach, U., Stevens, T., Kukla, G.J., Heller, F., William, D., McCoy, W. D., Oches, E.A., Buggle, B., Zöller, L., 2011. The last million years recorded at the Stari Slankamen (Northern Serbia) loess–palaeosol sequence: revised chronostratigraphy and long-term environmental trends. Quat. Sci. Rev. 30, 1142–1154. https://doi.org/10.1016/j.quascirev.2011.02.004.

Mirchink, G.F., 1936. Correlation of Continental Quaternary Deposits of the Russian Plain and Corresponding Deposits of the Caucasus and Ponto-Caspian. Leningrad-Moscow. In: Materials on the Quaternary Period of the USSR. To the Soviet Report. Delegations to the 3rd Conference of the International Association for the Study of the Quaternary Period, pp. 10–32 (In Russian).

Muhs, D.R., Bettis, E.A., 2003. Quaternary Loess-Paleosol Sequences as Examples of Climate-Driven Sedimentary Extremes. In: Chan, M.A., Archer, A.W. (Eds.), Extreme Depositional Environments: Mega End Members in Geologic Time, vol. 370. Geological Society of America Special Paper, Boulder, Colorado, pp. 53–74.

Murray, A.S., Thomsen, K.J., Masuda, N., Buylaert, J.P., Jain, M., 2012. Identifying well-bleached quartz using the different bleaching rates of quartz and feldspar luminescence signals. Radiat. Meas. 47 (9), 688–695. https://doi.org/10.1016/j.radmeas.2012.05.006.

Panin, P.G., Timireva, S.N., Konstantinov, E.A., Kalinin, P.I., Kononov, Y.M., Alekseev, A. O., Semenov, V.V., 2019. Plio-pleistocene paleosols: loess-paleosol sequence studied in the beregovoye section, the Crimean peninsula. Catena 172, 590–618. https://doi.org/10.1016/j.catena.2018.09.020.

Panin, P.G., Timireva, S.N., Morozova, T.D., Kononov, Y.M., Velichko, A.A., 2018. Morphology and micromorphology of the loess-paleosol sequences in the south of the East European Plain (MIS 1-MIS 17). Catena 168, 79–101. https://doi.org/10.1016/j.catena.2018.01.032.

Pécsi, M., 1990. Loess is not just the accumulation of dust. Quat. Int. 7–8, 1–21. https://doi.org/10.1016/1040-6182(90)90034-2.

Pilipenko, O.V., Sharonova, Z.V., Trubikhin, V.M., Abrahamsen, N., Moerner, N.-A., 2005. Paleomagnetic and petromagnetic investigations of rocks of the Pekla loess-soil section (Krasnodar territory) in the interval 240-55 ka. Izvestiya Phys. Solid Earth 41 (6), 492–501.

Pilipenko, O.V., Trubikhin, V.M., 2011. Paleomagnetic record in the Late Pleistocene loess-soil deposits of the Pekla section in the time interval 425-50 Ka. Izvestiya Phys. Solid Earth 47 (8), 686–697.

Porter, X., An, Z., 1995. Correlation between climate events in the north Atlantic and China during the last glaciation. Nature 375, 305–308. https://doi.org/10.1038/375305a0.

Potapov, I.I., Safronov, I.I., 1985. Relief, Geological Structure and Minerals of the North Caucasian Economic Region. Izd. Rostovskogo Universiteta. Rostov-na-Donu, p. 154 (In Russian).

Pye, K., 1995. The nature, origin and accumulation of loess. Quat. Sci. Rev. 14, 653–667. https://doi.org/10.1016/0277-3791(95)00047-X.

Ryskov, Y.G., Oleinik, S.A., Velichko, A.A., Nikolaev, V.I., Timireva, S.N., Nechaev, V.P., Panin, P.G., Morozova, T.D., 2008. Reconstruction of the paleotemperature and precipitation in the Pleistocene according to the isotope composition of humus and carbonates in loess on the Russian plain. Eurasian Soil Sci. 41 (9), 937–945. https://doi.org/10.1134/S1064229308090044.

Shardanov, A.N., Borukaev, Ch.B., 1968. The Taman peninsula and western Caucasus. In: North Caucasus. Part 1: Geological Description, vol. IX. Nedra, Moscow, pp. 594–606 (In Russian)Geology of the USSR.

Sizikova, A.O., Zykina, V.S., 2015. The dynamics of the late Pleistocene loess formation, Lozhok section, Ob loess plateau, SW Siberia. Quat. Int. 365, 4–14. https://doi.org/10.1016/j.quaint.2014.09.030.

Smalley, I.J., Markovic, S.B., Svircev, Z., 2011. Loess is [almost totally formed by] the accumulation of dust. Quat. Int. 240, 4–11. https://doi.org/10.1016/j.quaint.2010.07.011.

Stevens, T., Thomas, D.S.G., Armitage, S.J., Lunn, H.R., Lu, H., 2007. Reinterpreting climate proxy records from late Quaternary Chinese loess: a detailed OSL investigation. Earth Sci. Rev. 80 (1–2), 111–136. https://doi.org/10.1016/j.earscirev.2006.09.001.

Svitoch, A.A., Selivanov, A.O., Yanina, T.A., 1998. Paleogeographic Events of Ponto-Caspian and Mediterranean: Materials on Reconstruction and Correlation. MSU Publishing House, Moscow, p. 292.

Timireva, S.N., Velichko, A.A., 2006. Depositional environments of the Pleistocene loess-soil series inferred from sand grain morphoscopy – a case study of the East European Plain. Quat. Int. 152, 136–145. https://doi.org/10.1016/j.quaint.2005.12.013.

Velichko, A.A., Borisova, O.K., Zakharov, A.L., Kononov, Yu.M., Konstantinov, E.A., Kurbanov, R.N., Morozova, T.D., Panin, P.G., Timireva, S.N., 2017b. Landscape changes in the southern Russian plain in the late Pleistocene: a case study of the loess-soil sequence in the Azov Sea region. Izvestiya Rossiiskaya Akademii Nauk, seriya geograficheskaya 1, 74–83.

Velichko, A.A., Borisova, O.K., Kononov, Yu.M., Konstantinov, E.A., Kurbanov, R.N., Morozova, T.D., Panin, P.G., Semenov, V.V., Tesakov, A.S., Timireva, S.N., Titov, V. V., Frolov, P.D., 2017c. Reconstruction of late Pleistocene events in the periglacial area in the southern part of the East European Plain. Dokl. Earth Sci. 475 (2), 896–900.

Velichko, A.A., Morozova, T.D., Borisova, O.K., Timireva, S.N., Semenov, V.V., Kononov, Yu.M., Konstantinov, E.E., Kurbanov, R.N., Titov, V.V., Tesakov, A.S., 2012. Development of the steppe zone in Southern Russia based on the reconstruction from the loess-soil formation in the Don - Azov region. Dokl. Earth Sci. 445 (2), 999–1002.

Velichko, A.A., 1990. Loess-paleosol formation on the Russian plain. Quat. Int. 7–8, 103–114. https://doi.org/10.1016/1040-6182(90)90044-5.

Velichko, A.A., Catto, N.R., Kononov, M.Y., Morozova, T.D., Novenko, E.Yu., Panin, P.G., Ryskov, G.Y., Semenov, V.V., Timireva, S.N., Titov, V.V., Tesakov, A.S., 2009a. Progressively cooler, drier interglacials in southern Russia through the Quaternary: evidence from the Sea of Azov region. Quat. Int. 198 (1–2), 204–219. https://doi.org/10.1016/j.quaint.2008.06.005.

Velichko, A.A., Catto, N.R., Tesakov, A.S., Titov, V.V., Morozova, T.D., Semenov, V.V., Timireva, S.N., 2009b. Structural specificity of Pleistocene loess and soil formation of the southern Russian plain according to materials of Eastern Priazovie. Dokl. Earth Sci. 429, 1364–1368.

Velichko, A.A., Faustova, M.A., Pisareva, V.V., Gribchenko, Yu.N., Sudakova, N.G., Lavrentiev, N.V., 2011. Chapter 26 - Glaciations of the East European Plain: Distribution and Chronology. In: Ehlers, J., Gibbard, P.L., Hughes, P.D. (Eds.), Developments in Quaternary Sciences, vol. 15, pp. 337–359. https://doi.org/10.1016/B978-0-444-53447-7.00026-X.

Velichko, A.A., Kononov, Yu.M., Faustova, M.A., 2000. Geochronology, distribution, and ice volume on the earth during the last glacial maximum: inferences from new data. Stratigr. Geol. Correl. 8 (1), 1–12.

Velichko, A.A., Markova, A.K., Morozova, T.D., 1992. Loess-Paleosol Geochronology of the South-West Russian Plain on New Data. In: Quaternary Geochronology. Nauka, Moscow, pp. 28–33 (In Russian).

Velichko, A.A., Morozova, T.D., 2010. Basic features of Late Pleistocene soil formation in the East European Plain and their paleogeographic interpretation. Eurasian Soil Sci. 43, 1535–1546. https://doi.org/10.1134/S1064229310130120.

Velichko, A.A., Morozova, T.D., 2015. Main features of soil formation within the Pleistocene on the East European Plain and their paleogeographical. In: Kudeyarov, V.N., Ivanov, I.V. (Eds.), Evolution of Soil and Soil Cover. Theory, Diversity of Natural Evolution and Anthropogenic Transformations of Soil. GEOS, Moscow, pp. 321–337 (In Russian).

Velichko, A.A., Morozova, T.D., Pevzner, M.A., 1973a. Structure and age of loess and fossil soil horizons on the main terrace levels of the northern Azov region. Paleomagnetic Analyses in Studies of Quaternary Deposits and Volcano Formations. Nauka, Moscow, pp. 48–70 (In Russian).

Velichko, A.A., Morozova, T.D., Pevzner, M.A., Khalcheva, T.A., 1973b. Sequences of Loesses and Fossil Soils on Chaudian-Bakinian Deposits in the Taman Peninsula and Their Paleomagnetic Characteristics. In: Paleomagnetic Analyses in Studies of Quaternary Deposits and Volcano Formations. Nauka, Moscow, pp. 70–76 (In Russian).

Velichko, A.A., Yang, T., Alekseev, A.O., Borisova, O.K., Kalinin, P.L., Konishchev, V.N., Kononov, Yu.M., Konstantinov, E.A., Kurbanov, R.N., Panin, P.G., Rogov, V.V., Sarana, V.A., Timireva, S.N., Chubarov, I.G., 2017a. A comparative analysis of changing sedimentation conditions during the last interglacial-glacial macrocycle in the loess areas of the southern East European Plain (the Azov Sea region) and Central China (the Loess plateau). Geomorfologiya 1, 3–18. https://doi.org/10.15356/0435-4281-2017-1-3-18 (In Russian).

Zastrozhnov, A., Danukalova, G., Shick, S., van Kolfshoten, T., 2017. State of stratigraphic knowledge of Quaternary deposits in European Russia: unresolved

issues and challenges for further research. Quat. Int. 478, 4–26. https://doi.org/10.1016/j.quaint.2017.03.037.

Zubakov, V.A., 1988. Climatostratigraphic scheme of the Black Sea Pleistocene and its correlation with the oxygen-isotope scale and glacial events. Quat. Res. 29 (1), 1–24. https://doi.org/10.1016/0033-5894(88)90067-1.

Zykina, V.S., Zykin, V.S., 2008. The loess-soil sequence of the Brunhes Chron from West Siberia and its correlation to global and climate records. Quat. Int. 179 (1), 171–175. https://doi.org/10.1016/j.quaint.2007.10.010.